

SERBIAN JOURNAL OF ELECTRICAL ENGINEERING
Vol. 10, No. 2, June 2013, 275-291

UDK: 621.314.1:681.515

DOI: 10.2298/SJEE130114004B

Robust Sensorless Control of BLDC Motor using Second Derivative Function of the Sum of Terminal Voltages

Abdelali Boughaba¹, Mabrouk Chaabane², Said Benaggoune³

Abstract: This paper proposes a new sensorless control method for the speed and position control of a BLDC Motor. This sensorless drive technique calculates the commutations instants (duration of commutation) by deriving the sum of the terminal voltages of the motor ($\text{Sig}V_i$). Thus, it is possible to estimate the rotor position (and back EMF of the motor) by only using measurements of the stator line currents and voltages. The implantation of these detectors is easy and cheap. This method is quite robust across variations in stator resistance due to changes in temperature or frequency. With this method the motor can be started without needing the initial position of the rotor. This proposed method is validated through extensive simulations at different speeds, and a very satisfactory performance has been achieved.

Keywords: Sensorless, Drive, Control, Brushless DC Motor, Terminal Voltages, Trapezoidal Back EMF.

1 Introduction

Permanent magnet synchronous motors, and particularly those known as being without a collector (brushless motors), have an increasingly important use. This development is due to their high efficiency, high power density and large torque to inertia ratio [1]. Brushless DC (BLDC) motor is inherently electronically controlled, and requires rotor position information for the proper commutation of the current [2]. The techniques for control developed until now are numerous. Several among them are based on the detection of electromotive force waveforms (back EMF) [3]. The implantation of dedicated sensors is an operation which is extremely delicate and relatively expensive [4]. However the problems related to the cost and reliability of rotor position sensors have motivated researchers to develop the position-sensorless BLDC motor drive.

¹LRPI – Research Laboratory, Institute of Health and Industrial Safety, Batna University, El Hadj Lakhdar Campus, 05000 Batna, Algeria. E-mail: abdelali_boughaba@yahoo.fr

²LEB – Research Laboratory, Department of Electrical Engineering, Batna University, Chahid Med El Hadi Boukhlof, Batna 05000, Algeria. E-mail: mabrouk.chaabane@univ-batna.dz

³LSTE – Research Laboratory, Department of Electrical Engineering, Batna University, Chahid Med El Hadi Boukhlof, Batna 05000, Algeria. E-mail: s_benaggoune@yahoo.fr

Various techniques of control for the BLDC motor have been developed over the last few years. Among them are a control strategy based on the common DC signal [2], control by a new function of flux estimation [1], and a sensorless commutation integrated circuit (IC) for a BLDC motor [5].

This paper presents the basis of a new sensorless position estimation method by the application of a new concept. This technique is based on the derivative function of the sum of the stator phase voltages. The results validation has been carried out on a simulation model for the sensorless control of a BLDC motor.

Stabilization is taken into account by integrating a PI speed regulator.

2 Basic Equations of a BLDC Motor

2.1 Synchronous motor (PMSM) model

For controlling and analysing a BLDCM, the structure of a permanent magnet synchronous motor (PMSM) is usually used. That means that the distribution of the magnetic field is taken as sinusoidal [6].

The circuit equations are given by:

$$\dot{\mathbf{X}} = \mathbf{A}\mathbf{X} + \mathbf{B}\mathbf{U}, \quad (1)$$

where $\mathbf{X} = [I_d \quad I_q \quad \omega \quad \theta]^T$, and

$$\begin{aligned} \frac{dI_d}{dt} &= \frac{V_d}{L} - \frac{I_d}{\tau} + \omega I_q, \\ \frac{dI_q}{dt} &= \frac{V_q}{L} - \frac{I_q}{\tau} - \omega I_d - \frac{K_e}{L} \omega, \\ \frac{d\omega}{dt} &= \frac{pK_e}{J} I_q - \frac{f}{J} \omega - \frac{p}{J} T_L, \\ \frac{d\theta}{dt} &= \omega, \end{aligned}$$

with $\mathbf{Y} = \mathbf{C}\mathbf{X}$, where $\mathbf{Y} = [I_d \quad I_q]^T$, $\mathbf{C} = \begin{bmatrix} 1 & 0 & 0 & 0 \\ 0 & 1 & 0 & 0 \end{bmatrix}$, and

V_d, V_q, I_d, I_q – voltages and currents on a (d,q) frame,

T_L – torque load,

ω – electrical angular velocity,

K_e – factor torque,

L – inductance,

R – resistance,

τ – electric time-constant.

2.1 Model of BLDC Motor (Trapezoidal Back EMF Form)

A BLDC motor with trapezoidal back EMF is conventionally modelled in the stationary frame using three phases, a , b , c , because EMFs are difficult to transform into the d-q reference frame.

We consider a motor with a permanent magnet mounted on the surface (without saliency effects).

Fig. 1 gives the equivalent circuit of the BLDCM.

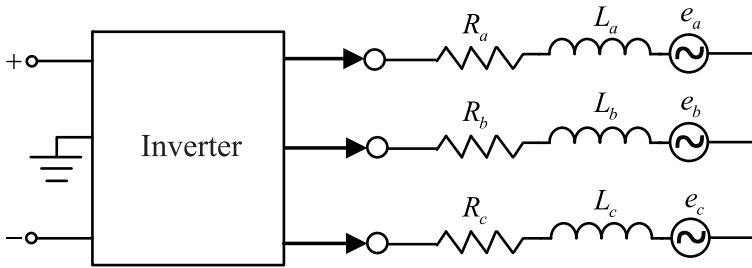


Fig. 1 – BLDC motor equivalent circuit.

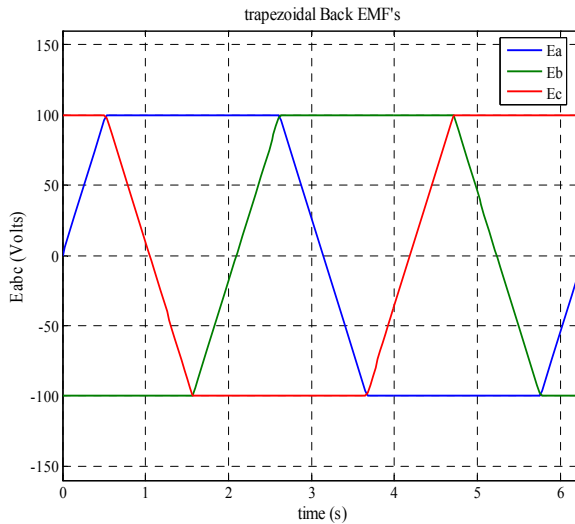


Fig. 2 – Trapezoidal back EMF.

The general voltage equations of the BLDC motor are given as follows:

$$\underline{v} = [\mathbf{R}]i + [\mathbf{L}]\frac{di}{dt} + \underline{e}, \quad (2)$$

where \mathbf{R} is the stator resistance per phase:

$$\mathbf{R} = \begin{bmatrix} R & 0 & 0 \\ 0 & R & 0 \\ 0 & 0 & R \end{bmatrix},$$

\mathbf{L} is the matrix of inductance (L_s , M : self and mutual inductance):

$$\mathbf{L} = \begin{bmatrix} L_s & -M & -M \\ -M & L_s & -M \\ -M & -M & L_s \end{bmatrix}$$

and $\underline{e} = [e_a \ e_b \ e_c]^T$ is the vector of the trapezoidal back EMF (Fig. 2).

Equation (2) becomes:

$$\frac{d}{dt} \begin{bmatrix} I_a \\ I_b \\ I_c \end{bmatrix} = \begin{bmatrix} \frac{1}{L_T} & 0 & 0 \\ 0 & \frac{1}{L_T} & 0 \\ 0 & 0 & \frac{1}{L_T} \end{bmatrix} \left\{ \begin{bmatrix} V_{an} \\ V_{bn} \\ V_{cn} \end{bmatrix} - \begin{bmatrix} R & 0 & 0 \\ 0 & R & 0 \\ 0 & 0 & R \end{bmatrix} \begin{bmatrix} I_a \\ I_b \\ I_c \end{bmatrix} - \begin{bmatrix} e_{an} \\ e_{bn} \\ e_{cn} \end{bmatrix} \right\}, \quad (3)$$

where $L_T = L_s + M$.

The mechanical equation of motion is:

$$J \frac{d\omega_r}{dt} = T_{em} - T_l - f\omega_r, \quad (4)$$

with:

$$T_{em} = \frac{1}{\omega_r} (e_{an}i_a + e_{bn}i_b + e_{cn}i_c), \quad (5)$$

where:

ω_r – mechanical speed [rad/s],

T_l – torque load [N m],

J – motor shaft and load inertias [kg m²]

f – frictional damping coefficient [N m s/rad m],

T_{em} – electromagnetic torque [Nm].

In a BLDC motor without a neutral connection we have:

$$I_a + I_b + I_c = 0, \quad (6)$$

(Every time we have one phase the current is set to zero, and the two others are opposed.)

3 Proposed Method for Estimation of Rotor Position

The proposed method is based on the decomposition of the phase currents and back EMF by the Fourier transformation.

The decomposition gives:

$$\begin{aligned}
 i_a(\theta_e) &= \frac{4I_m}{\pi} \sum_n \frac{1}{n} \cos n \frac{\pi}{6} \sin n\theta_e, \\
 i_b(\theta_e) &= -\frac{2I_m}{\pi} \sum_n \frac{1}{n} \left[\left(\sin n \frac{\pi}{6} + \sin n \frac{\pi}{2} \right) \cos n\theta_e + \cos n \frac{\pi}{6} \sin n\theta_e \right], \\
 i_c(\theta_e) &= \frac{2I_m}{\pi} \sum_n \frac{1}{n} \left[\left(\sin n \frac{\pi}{6} + \sin n \frac{\pi}{2} \right) \cos n\theta_e + \cos n \frac{\pi}{6} \sin n\theta_e \right].
 \end{aligned} \quad (7)$$

The equations of the Fourier transformations of a trapezoidal back EMF are given as follows:

$$\begin{aligned}
 e_a(\theta_e) &= \frac{24E}{\pi^2} \sum_{n=1,2,3,\dots} \frac{1}{n^2} \sin n \frac{\pi}{6} \sin n\theta_e, \\
 e_b(\theta_e) &= \frac{12E}{\pi^2} \sum_{n=1,2,3,\dots} \frac{1}{n^2} \left[\left(\sin n \frac{\pi}{6} - \sin n \frac{\pi}{2} \right) \sin n\theta_e - \cos n \frac{\pi}{6} \cos n\theta_e \right], \\
 e_c(\theta_e) &= \frac{12E}{\pi^2} \sum_{n=1,2,3,\dots} \frac{1}{n^2} \left[\left(\sin n \frac{\pi}{6} - \sin n \frac{\pi}{2} \right) \sin n\theta_e + \cos n \frac{\pi}{6} \cos n\theta_e \right],
 \end{aligned} \quad (8)$$

where:

$$\begin{aligned}
 E &= \lambda_f \omega_e, \\
 \theta_e &= p\theta, \\
 \omega_e &= p\omega,
 \end{aligned} \quad (9)$$

θ_e – electrical rotor position,

ω_e – electrical speed,

λ_f – field flux linkage,

p – pole pair number.

In order to estimate the rotor position it is necessary to use system (2), which gives:

$$\sum_{k=a,b,c} V_k = R_s \sum_{k=a,b,c} i_k + L \frac{d}{dt} \sum_{k=a,b,c} i_k + \sum_{k=a,b,c} e_k, \quad (10)$$

where:

$$\sum_{k=a,b,c} i_k = 0.$$

Thus, (11) combined with the above condition gives:

$$\sum_{k=a,b,c} V_k = \sum_{k=a,b,c} e_k . \quad (11)$$

From (3) we obtain:

$$\sum_{k=a,b,c} e_k = \begin{cases} 0 & \text{for } n = 1, 5, 7, 11 \\ 0,81E \sin 3\theta_e & \text{for } n = 3 \\ -0,09E \sin 9\theta_e & \text{for } n = 9 \\ 0.0324E \sin 15\theta_e & \text{for } n = 15 \end{cases} \quad (12)$$

Fig. 3 illustrates the decomposition of the sum of back EMFs, which is clearly nonzero.

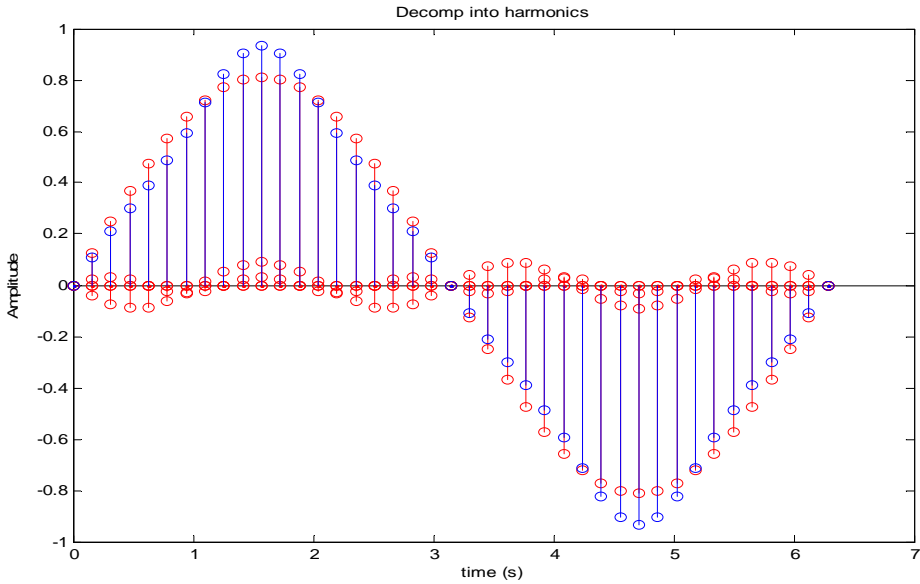


Fig. 3 – Sum of back EMF decomposition.

It is clear from Fig. 3 that the sum of the back EMFs contains information about the rotor position.

From the simulation we can see in Fig. 4 that the error between the sum of the terminal voltages ($\sum V_i$) and sum of the back EMFs ($\sum E_i$) is nearly zero.

Thus we can use the sum of terminal voltages, which is exactly equal to the sum of back EMFs, to estimate the rotor position. The proposed method is based on the second derivation of the function of the sum of terminal voltages:

$$F = \frac{d^2 \text{sig} V_i}{dt^2} .$$

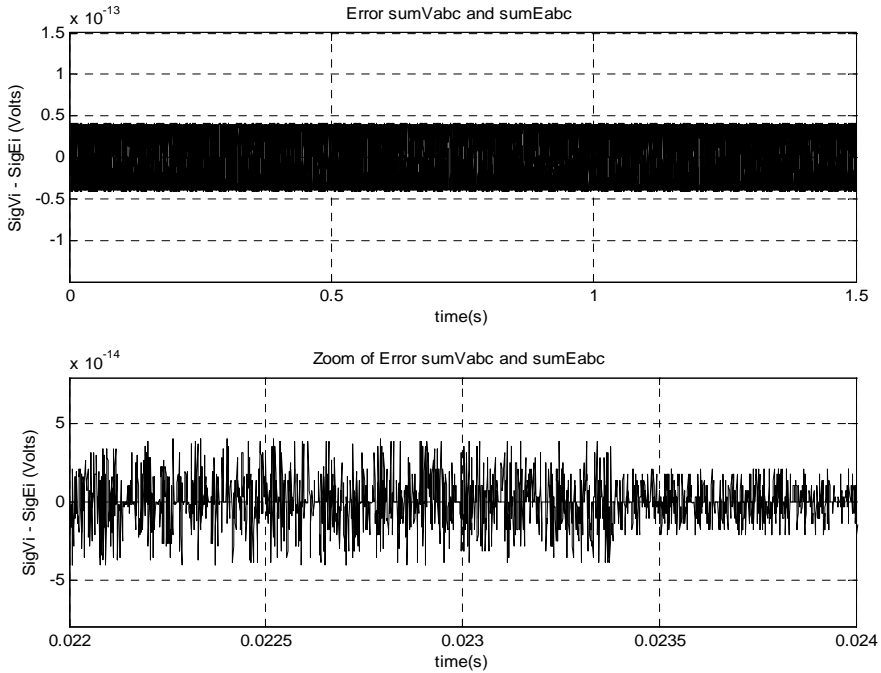


Fig. 4 – Error $\text{Sum}V_i - \text{Sum}E_i$.

Figs. 5a and 5b show the structure of the block diagram, giving the principle of the sensorless commutation of BDCM control. The block (time calculation switching) generates the control signal of the inverter (conditions given by **Table 1** are taken into account). Signals from function F require processing and adaptation. The maximum value of the reference current is obtained from the PI block. The block (current control) is a hysteresis current controller.

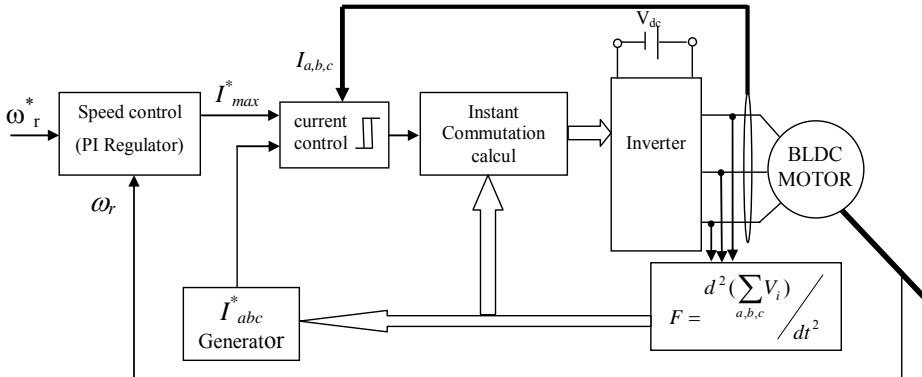


Fig. 5a – Block diagram of BDCM control with sensorless drive.

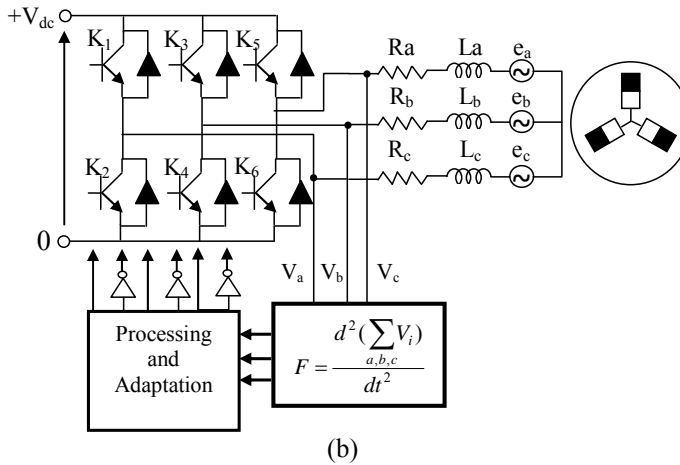


Fig. 5b – Description of inverter block with BDCM.

4 BLDC Motor Starting Mode

The procedure for starting a sensorless drive for the BDCM is so difficult, because the rotor has a permanent magnet and its position is unknown. In the references we can find several possible procedures for starting a BDCM [7]:

- 1 – auxiliary sensor;
- 2 – open loop control;
- 3 – specific gate pattern;
- 4 – arbitrary starting;
- 5 – salient-pole motor;

The arbitrary start-up is the method chosen for this simulation, but in practice this method cannot be achieved because, in some cases, it may be accompanied by temporary reversed rotation.

5 BLDC Motor Parameters (Bosch SE-B2.040.060)

Parameters of the BDCM used in the simulations are all in real units [6]:

$R = 1.43 \Omega$, $L_w = 9.4 \cdot 10^{-3} \text{ H}$, $\Phi_f = 0.2158 \text{ Wb}$, $J = 1.5 \cdot 10^{-3} \text{ kgm}^2$,
 $f = 2 \cdot 10^{-3} \text{ Ns/rad}$, $p = 2$ pole pairs, $K_t = 0.41 \text{ Nm/A}$,
 Rated current = 9.7 A, Rated voltage = 380 V, Peak current = 58 A.

6 Sensitivity Study and Simulation Results


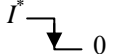
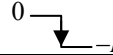
As described in the block diagram (Fig. 5), the speed regulation provides the module of the current phase.

The new proposed sensorless drive has been successfully simulated on a BLDC Motor with the parameters as given above (Section 5).

In this section, the effectiveness of the proposed method of sensorless control for a BLDC motor is verified by computer simulation. Several tests were conducted to check the performance of the proposed method. In all the figures the time axis is scaled in seconds.

The procedure for energizing the inverter gates are as follows in **Table 1**.

Table 1
Commutation Sequences.

	FG	I_k	Then $I_k (k = a, b, c)$
If	> 0	0	
If	> 0	> 0	
If	< 0	0	
If	< 0	< 0	
If	> 0	< 0	I^*
If	< 0	> 0	I^*

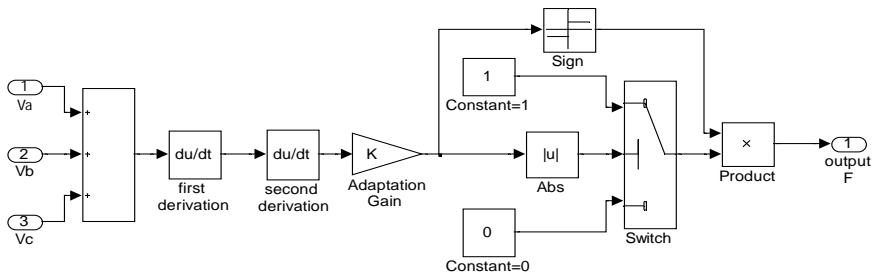


Fig. 6 – *Block scheme of processing circuit.*

Fig. 6 illustrates the block diagram scheme for the processing signals $(d^2(\text{Sig}V_i)/dt^2)$ which contains a ripple near zero, where V_a , V_b and V_c are the measured terminal voltages and F gives the command signals from the second derivative function of $\text{Sig}V_i$. K is an attenuation coefficient ($K < 1$) of the second derivative function of $\text{Sig}V_i$.

6.1 Variation in speed and load torque application

Fig. 7 presents the speed response and electrical rotor position for the variable speed reference. The reaction is quiet, fast and of high accuracy.

Moreover, in Fig. 8 the tracking performances were improved when a load torque is suddenly applied and removed. However, the torque of the BLDC motor contains a ripple.

These properties make this new method suitable for applications in which accuracy and speed are required.

6.2 Test under constant speed

Fig. 9 shows the speed response, rotor position, sum of three terminal voltages ($\text{Sig}V_i$), back EMF phase currents, and the crossing zero signal (corresponding to signals necessary to energise the gates).

The sequence from the back EMF zero crossing commutation is clearly demonstrated. As we can see, the commutation will occur approximately 30 electric degrees after the zero crossing of the back EMF.

6.3 Variation in stator resistance

The effect of changes in the stator resistance on the new method is examined. Fig. 10 describes the performance of the new method for a wide variation of stator resistances, and illustrates the results of the simulation with a reference speed equal to 100 rad/s, load torque equal to 2 Nm and two values for the stator resistance ($R = R_n$ and $R = R_n + 150\% R_n$). This variation in resistance will not significantly affect the performance of this new method. From this figure we determine a delay time of 400 μs .

Fig. 9 demonstrates the accuracy of the commutation timing. This method of calculation of commutation instants (zero crossing) has a very good resolution, particularly at low speed when the back EMF amplitude is very low.

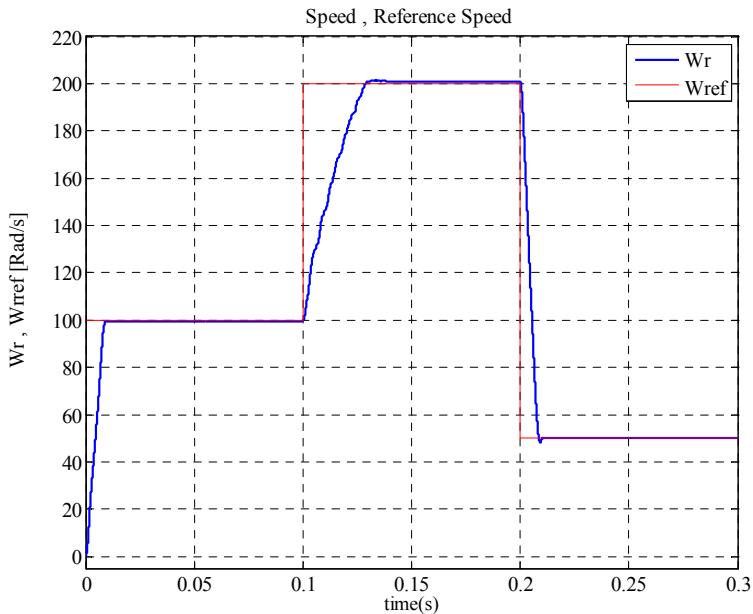


Fig. 7a – Response obtained with variable reference speed: Speed, Reference Speed.

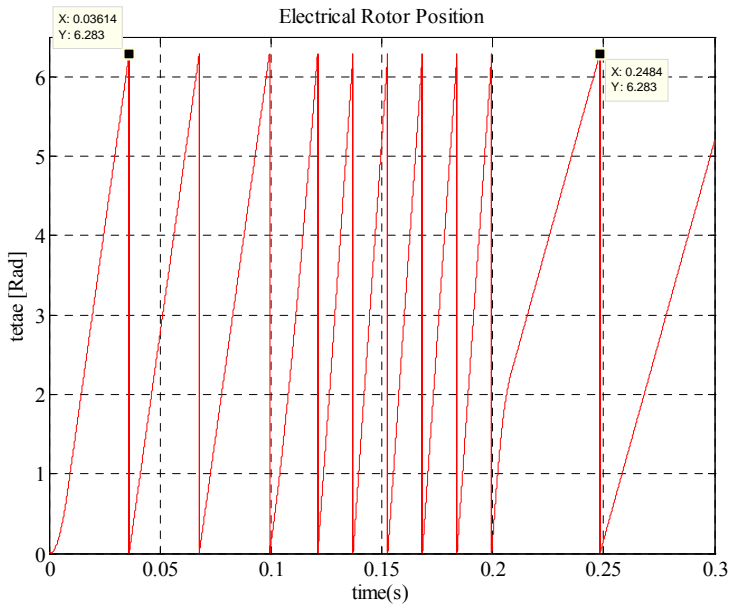


Fig. 7b – Response obtained with variable reference speed: Electrical rotor position.

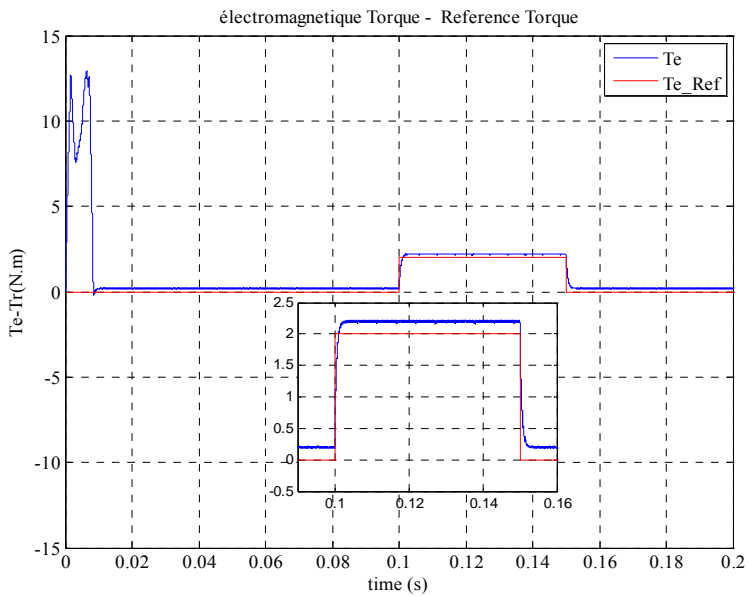


Fig. 8 – Response under load torque charge.

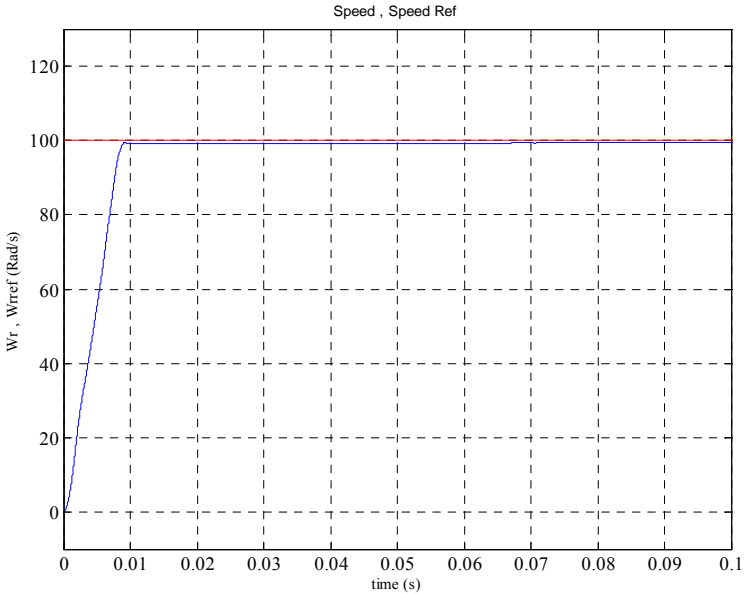


Fig. 9a – Response of drive under constant speed (with zoom): W_r, W_{ref} .

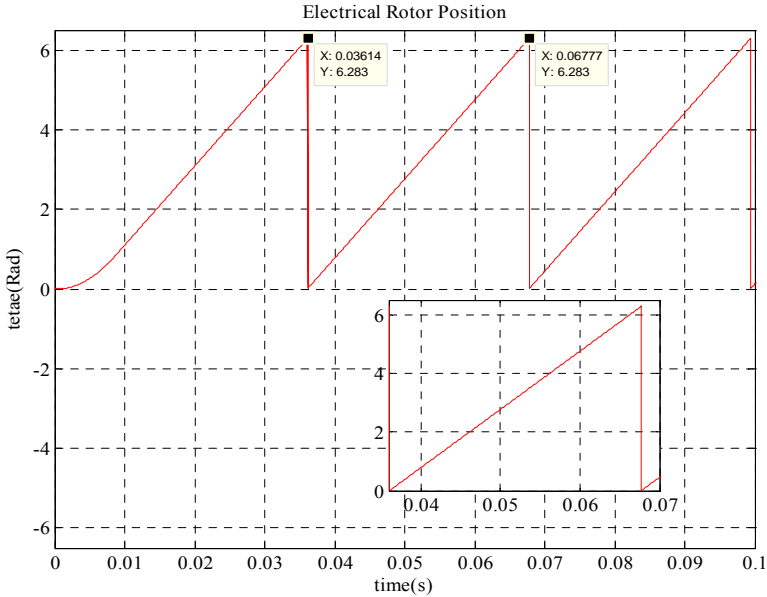


Fig. 9b – Response of drive under constant speed (with zoom): $teta_e$.

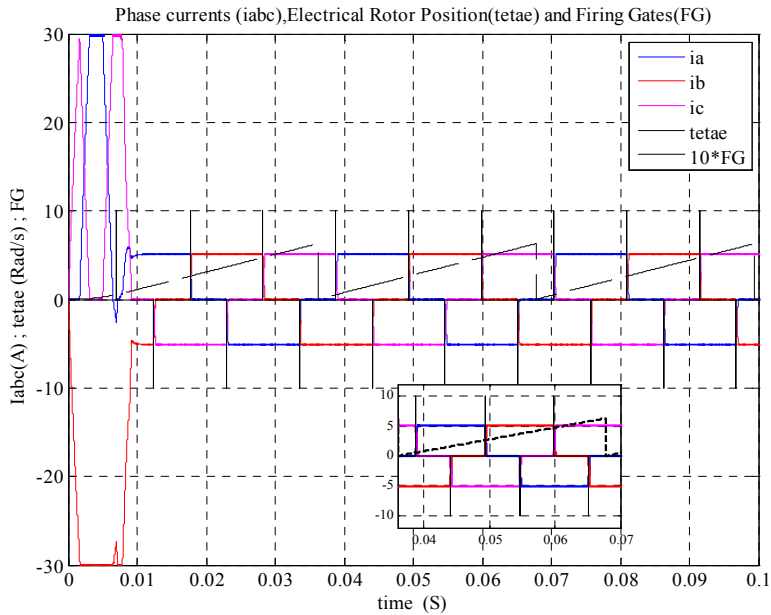


Fig. 9c – Response of drive under constant speed (with zoom): i_{abc} , $tetae$, FG.

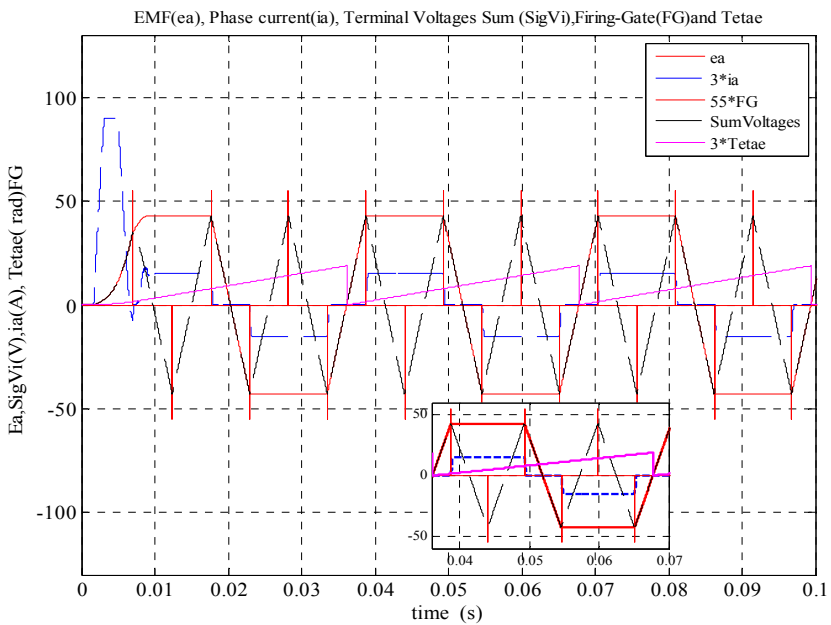


Fig. 9d – Response of drive under constant speed (with zoom): e_a , i_a , $tetae$, $SigV_i$, FG.

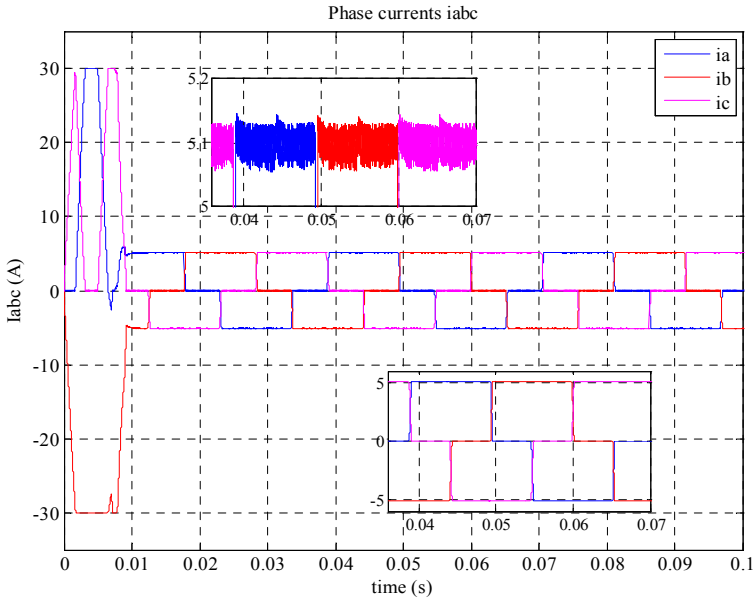


Fig. 9e – Response of drive under constant speed (with zoom): i_{abc} .

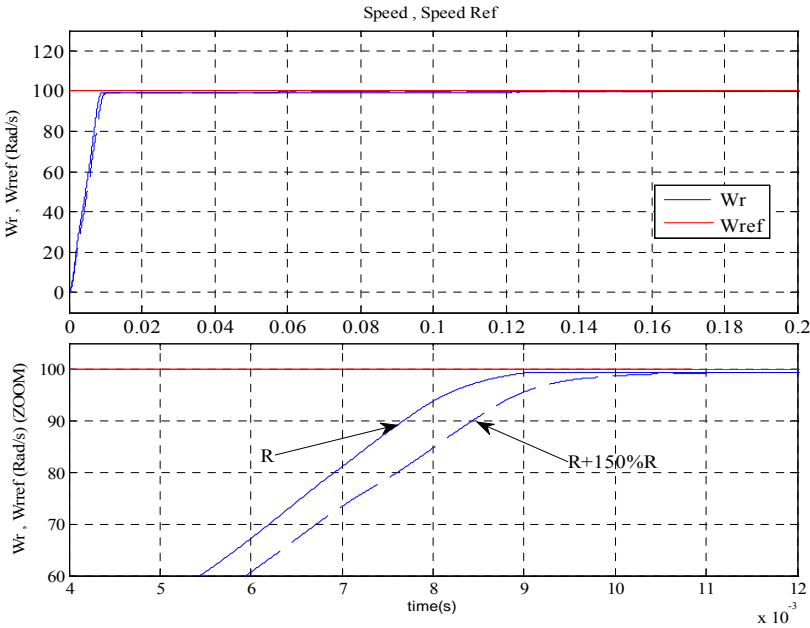


Fig. 10a – Response under stator resistance change ($R = R_n, R = R_n + 1.5R_n$): W_r, W_{ref} .

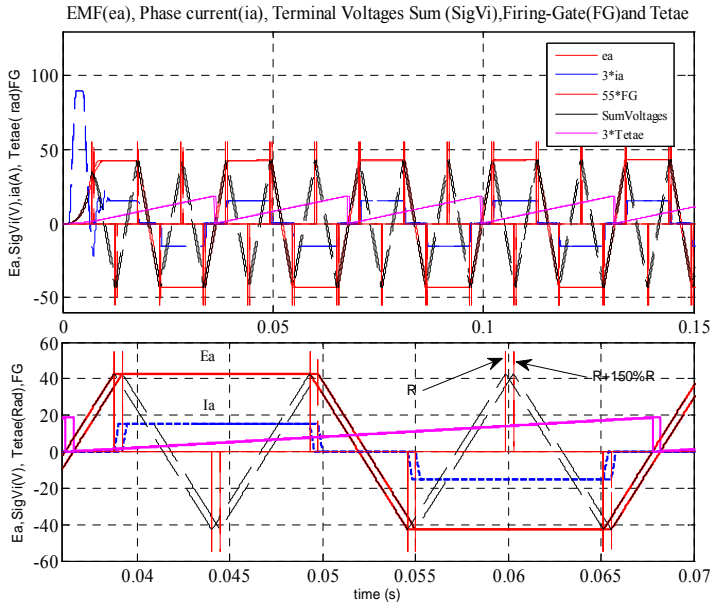


Fig. 10b – Response under stator resistance change ($R = R_n$, $R = R_n + 1.5R_n$): ea, ia, tetae, SigV_i, FG (with zoom).

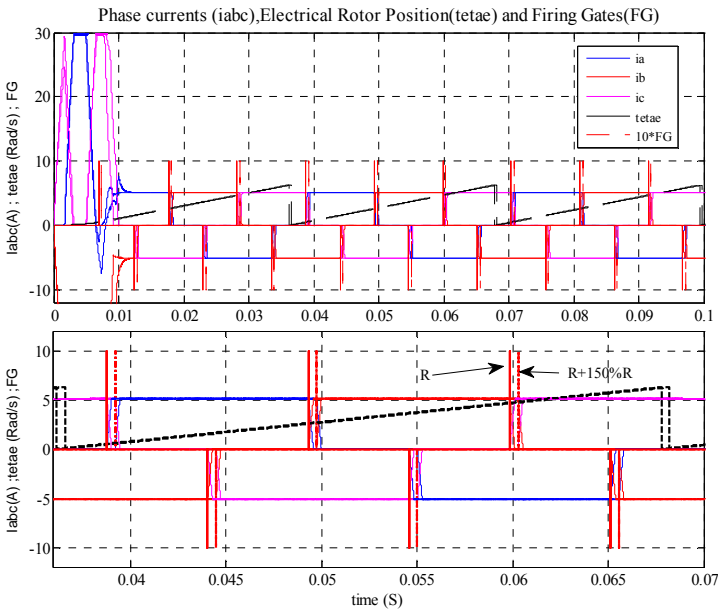


Fig. 10c – Response under stator resistance change ($R = R_n$, $R = R_n + 1.5R_n$): iabc, tetae, FG.

8 Conclusion

A novel robust sensorless drive for a BLDC motor by the calculation of commutation instants using the second derivative function of the sum of terminal voltages has been presented. This is a different way to use the information contained in the terminal voltages. The test results, by simulation, verify the analysis and demonstrate the advantages of this new method. These results show clearly that the true zero crossing back EMF is exactly contained in the sum of terminal voltages. It was shown that the new method possesses good robustness against parameter variation, in this case stator resistance. $\text{Sig}V_i$ has a few discrete values, and we note that $\text{Sig}V_i$ represents the sum of the terminal voltages averaged over each PWM cycle, and that the measured voltages in real application should be filtered. Nevertheless, as with most sensorless methods, the motor start up procedure still has to be integrated.

9 References

- [1] T. Kim, M. Ehsani: Sensorless Control of the BLDC Motors From Near-zero to High Speeds, IEEE Transactions on Power Electronics, Vol. 19, No. 6, Nov. 2004, pp. 1635 – 1645.
- [2] C.L.P. Swamy, B. Singh, B.P. Singh: Dynamic Performance of a Permanent Magnet Brushless DC Motor Powered by PV Array For Water Pumping, Solar Energy Materials and Solar Cells, Vol. 36, No. 2, Feb. 1995, pp. 187 – 200.
- [3] N. Matsui: Sensorless PM Brushless DC Motor Drives, IEEE Transactions on Industrial Electronics, Vol. 43, No. 2, April 1996, pp. 300 – 308.
- [4] B. Terzic, M. Jadric: Design and Implementation of the Extended Kalman Filter for the Speed Rotor Position Estimation of Brushless DC Motor, IEEE Transactions on Industrial Electronics, Vol. 48, No. 6, Dec, 2001, pp. 1065 – 1073.
- [5] G.H. Jang, J.H. Park, J.H. Chang: Position Detection and Start-up Algorithm of a Rotor in a Sensorless DLDC Motor using Inductance Variation, IEE Proceedings -Electric Power Applications, Vol. 149, No. 2, March 2002, pp. 137 – 142.
- [6] M.T. Wishart, R.G. Harley, G. Diana: The Application of Field Oriented Control to the Brushless DC Machine, 4th European Conference on Power Electronics and Applications, Firenze, Italy, 03 – 06 Sept. 1991, Vol. 3, pp. 629 – 634.
- [7] J.X. Shen, Z.Q. Zhu, D. Howe: Sensorless Flux-weakening Control of Permanent Magnet Brushless Machines using Third Harmonic Back EMF, IEEE Transactions on Industry Applications, Vol. 40, No. 6, Nov/Dec. 2004, pp. 1629 – 1636.
- [8] L.W. Dixon, I.A. Leal: Current Control Strategy for Brushless DC Motors Based on a Common DC Signal, IEEE Transactions on Power Electronics, Vol. 17, No. 2, March 2002, pp. 232 – 240.
- [9] K.Y. Cheng, Y.Y. Tzou: Design of a Sensorless Commutation IC for BLDC Motors, IEEE Transactions on Power Electronics, Vol. 18, No. 6, Nov. 2003, pp. 1365 – 1375.
- [10] J. Figueroa, C. Brocart, J. Cros, P. Viarouge: Simplified Simulation Methods for Polyphase Brushless DC Motors, Mathematics and Computers in Simulation, Vol. 63, No. 3-5, Nov. 2003, pp. 209 – 224.

- [11] P.M. Pelczewski, U.H. Kunz: The Optimal Control of a Constrained Drive System with Brushless DC Motor, IEEE Transactions on Industrial Electronics, Vol. 37, No. 5, Oct, 1990, pp. 342 – 348.
- [12] M. Tursini, R. Petrella, F. Parasiliti: Initial Rotor Position Estimation Method for PM Motors, IEEE Transactions on Industry Applications, Vol. 39, No. 6, Nov/Dec. 2003, pp. 1630 – 1640.
- [13] Z. Zheng, Y. Li, M. Fadel: Sensorless Control of PMSM based on Extended Kalman Filter, 12th European Conference on Power Electronics and Applications, Aalborg, Denmark, 02 – 05 Sept. 2007.
- [14] B.K. Lee, M. Ehsani: Advanced BLDC Motor Drive for Low Cost and High Performance Propulsion System in Electric and Hybrid Vehicles, 4th IEEE International Electric Machines and Drives Conference, Cambridge, MA, USA, 17 – 20 June 2001, pp. 246 – 251.
- [15] I. Colak, M. Sahin: Sensorless Control of a Brushless DC Motor using a Self-tuning PID, International Symposium on Power Electronics, Electrical Drives, Automation and Motion, Sorrento, Italy, 20 – 22 June 2012, pp. 1057 – 1062.
- [16] T.L. Chem, P.L. Pan, Y.L. Chem, D.M. Tsay: Sensorless Speed Control of BLDC Motor using Six Step Square Wave and Rotor Position Detection, 5th IEEE Conference on Industrial Electronics and Applications, Taichung, Taiwan, 15 – 17 June 2010, pp. 1358 – 1362.
- [17] D. Makiela: Sensorless Control of High-speed PM BLDC Motor, International Symposium on Industrial Electronics, Gdansk, Poland, 27 – 30 June 2011, pp. 722 – 727.